

ground state  $\text{Ru}(\text{NH}_3)_6^{2+}$ . Thus, both the excess Franck-Condon energy and the high-spin-low-spin energy difference in  $\text{Co}(\text{NH}_3)_6^{3+}$  are likely to account for our estimated difference in the CT excitation energies in the  $\text{Ru}(\text{NH}_3)_6^{3+}, \text{X}^-$  and  $\text{Co}(\text{NH}_3)_6^{3+}, \text{X}^-$  ion pairs.

In conclusion, one may say that the absence of absorption lines in the visible region in the spectrum of the  $\text{Ru}(\text{NH}_3)_6^{3+}$  free ion and the relatively low excitation energies for the CT transitions of its ion pairs make this complex an excellent ion for spectrophotometric investigations of ion pairs.

**Registry No.**  $\text{Ru}(\text{NH}_3)_6^{3+}, \text{Cl}^-$ , 53293-35-9;  $\text{Ru}(\text{NH}_3)_6^{3+}, \text{Br}^-$ , 53293-36-0;  $\text{Ru}(\text{NH}_3)_6^{3+}, \text{I}^-$ , 53293-37-1.

## References and Notes

- (1) E. Rabinowitch, *Rev. Mod. Phys.*, **14**, 112 (1942).
- (2) M. Linhard, *Z. Elektrochem.*, **50**, 224 (1944).
- (3) M. G. Evans, N. S. Hush, and N. Uri, *Quart. Rev., Chem. Soc.*, **6**, 186 (1952).
- (4) D. Waysbort and G. Navon, *J. Phys. Chem.*, **77**, 960 (1973).
- (5) D. Waysbort and G. Navon, *Chem. Commun.*, 1410 (1971).
- (6) T. J. Meyer and H. Taube, *Inorg. Chem.*, **7**, 2369 (1968).
- (7) L. Heck, *Inorg. Nucl. Chem. Lett.*, **7**, 701 (1971).
- (8) R. A. Robinson and R. H. Stokes, "Electrolyte Solutions," 2nd ed, Butterworths, London, 1959.
- (9) "Handbook of Chemistry and Physics," 51st ed, Chemical Rubber Publishing Co., Cleveland, Ohio, 1969.
- (10) The distance of closest approach for the  $\text{Ru}(\text{NH}_3)_6^{3+}, \text{I}^-$  ion pair was estimated by adding 0.17 Å to the cobalt-iodide smallest distance in  $\text{Co}(\text{NH}_3)_6^{3+}, \text{I}^-$  crystals<sup>11</sup> and for the chloride and bromide ion pairs by correcting for their corresponding ionic radii.
- (11) K. Meisel and W. Tiedje, *Z. Anorg. Allg. Chem.*, **164**, 223 (1927).
- (12) M. G. Evans and G. H. Nancollas, *Trans. Faraday Soc.*, **49**, 363 (1953).
- (13) See footnote 16 in ref 4.
- (14) R. Fuoss, *J. Amer. Chem. Soc.*, **80**, 5059 (1958).
- (15) H. Taube, cited as a private communication by J. A. Armor, *J. Inorg. Nucl. Chem.*, **35**, 2067 (1973).
- (16) H. Elsbernd and J. K. Beattie, *Inorg. Chem.*, **7**, 2468 (1968).
- (17) M. G. Evans and N. Uri, *Symp. Soc. Exp. Biol.*, **5**, 130 (1951).
- (18) J. Jortner, B. Raz, and G. Stein, *J. Chem. Phys.*, **34**, 1455 (1961).
- (19) J. Jortner and A. Treinin, *Trans. Faraday Soc.*, **58**, 1503 (1962).
- (20) C. E. Moore, *Nat. Bur. Stand. (U. S.), Circ.*, No. 467 (1958).
- (21) H. Yakoyama and H. Yamatera, *Bull. Chem. Soc. Jap.*, **44**, 1725 (1971).
- (22) J. F. Endicott and H. Taube, *J. Amer. Chem. Soc.*, **86**, 1686 (1964).
- (23) J. O'M. Bockris and B. E. Conway, Ed., "Modern Aspects of Electrochemistry," Vol. 1, Plenum Press, New York, N. Y., 1969, p 52.

Contribution from the Department of Chemistry,  
North Carolina State University, Raleigh, North Carolina 27607

## Cryogenic Excited-State Fine Structure of $[\text{Ni}(\text{NH}_3)_6]\text{A}_2$ and Magnetic Circular Dichroism Temperature Dependence of ${}^3\text{T}_{1g}(\text{t}_{2g}^5\text{e}_g^3)^1$

D. J. HAMM and A. F. SCHREINER\*

Received July 1, 1974

AIC40428L

Seven compounds of hexaamminenickel(II),  $[\text{Ni}(\text{NH}_3)_6]\text{A}_2$ , or the deuterated  $d_{18}$  analogs,  $[\text{Ni}(\text{ND}_3)_6]\text{A}_2$ , where  $\text{A}^- = \text{Cl}^-, \text{Br}^-, \text{I}^-, \text{ClO}_4^-$ , or  $\text{PF}_6^-$ , were studied by means of electronic absorption and magnetic circular dichroism (MCD) techniques at several temperatures (ca. 12–300°K). The absorption spectra in the d-d excitation region of six parity-forbidden bands permitted the observation of numerous vibronic progressions of the  $(\text{NiN}_6)$  skeletal normal modes and the symmetric stretching mode,  $\nu_s(\text{N-H})$ , which are modes of the electronic excited states. These are progressions of  $a_{1g}$  or  $e_g$  built on  $t_{1u}$  and  $t_{2u}$  modes. The temperature-dependent MCD spectra through  ${}^3\text{T}_{1g}(\text{t}_{2g}^5\text{e}_g^3)$  experimentally confirm the earlier suggestion that second-order spin-orbit coupling is important in the ground state  ${}^3\text{A}_{2g}(\text{t}_{2g}^6\text{e}_g^2)$  so as to give this state angular momentum from the excited state  ${}^3\text{T}_{2g}(\text{t}_{2g}^5\text{e}_g^3)$ . Finally, the band position of  ${}^3\text{A}_{2g} \rightarrow {}^1\text{A}_{1g}(\text{t}_{2g}^6\text{e}_g^2)$  is an excellent probe for the interaction between the lattice counterion and the complex ion  $[\text{Ni}(\text{NH}_3)_6]^{2+}$ .

## Introduction

The most recent report<sup>2</sup> dealing with the nature of electronic excited states of the important parent complex ion hexaamminenickel(II), or  $[\text{Ni}(\text{NH}_3)_6]^{2+}$ , contained descriptions of vibronic structural features on two d-d excitations,  ${}^3\text{A}_{2g} \rightarrow {}^3\text{T}_{1g}$  and  ${}^1\text{A}_{1g}$ , between ca. 600 nm ( $16,670 \text{ cm}^{-1}$ ) and 430 nm ( $23,260 \text{ cm}^{-1}$ ). This was observed at 80°K for the  $\text{Cl}^-$  and  $\text{ClO}_4^-$  salts of the complex ion and complemented ambient room-temperature solution spectra measured previously by others.<sup>3</sup> The present paper reports on newly observed vibronic structure, measured between 12 and 80°K, with distinct vibronic progressions on  ${}^3\text{T}_{2g}(\text{t}_{2g}^5\text{e}_g^3; {}^3\text{F})$ ,  ${}^3\text{T}_{1g}(\text{t}_{2g}^5\text{e}_g^3; {}^3\text{F})$ ,  ${}^1\text{E}_g(\text{t}_{2g}^6\text{e}_g^2; {}^1\text{D})$ ,  ${}^1\text{A}_{1g}(\text{t}_{2g}^6\text{e}_g^2; {}^1\text{G})$ ,  ${}^1\text{T}_{2g}(\text{t}_{2g}^4\text{e}_g^4; {}^1\text{D})$ , and  ${}^1\text{T}_{1g}(\text{t}_{2g}^5\text{e}_g^3; {}^1\text{G})$  which represent intra- as well as interconfigurational excitations. Some of the identifications of vibronic progressions were substantiated by preparing and studying the deuterated  $d_{18}$  complex,  $[\text{Ni}(\text{ND}_3)_6](\text{PF}_6)_2$ . In all, seven salts were studied, and the counterions were  $\text{Cl}^-, \text{Br}^-, \text{I}^-, \text{PF}_6^-$ , and  $\text{ClO}_4^-$ .

It was also possible experimentally to substantiate some suggestions made by Harding, Mason, Robbins, and Thomson<sup>4</sup>

about the MCD spectrum of  $[\text{Ni}(\text{NH}_3)_6]^{2+}$ ; i.e., we measured the MCD spectra at 18 and 27°K of  $[\text{Ni}(\text{NH}_3)_6]\text{Cl}_2$ . The latter data contribute importantly to the understanding of excited-state structure of the hexaammine.

## Experimental Section

**1. Instrumentation.** MCD spectra were obtained with a JASCO spectropolarimeter (Model ORD/UV/CD-5 with the SS-20 electronics modification). Low temperatures for MCD were attained by throttling vapors from a liquid helium reservoir past the sample. Near-ir, far-ir, and Raman spectra were measured on Perkin-Elmer 521, Perkin-Elmer FIS-3, and Jarrell-Ash 25-100 instruments (4880-Å Ar laser line), respectively. Low-temperature electronic absorption spectra were obtained by using an all-glass exchange-gas dewar and an all-glass dewar whose internal compartment and sample are cooled by throttling vapors from a liquid helium reservoir into it. Au-Cu vs. Cu and constantan vs. copper thermocouples were used following their calibration. The matrices of the crystalline samples were either KBr disks or Kel-F mulls.

**2. Compounds.** The syntheses of  $[\text{Ni}(\text{NH}_3)_6]\text{A}_2$  complexes, where  $\text{A}^- = \text{Cl}^-, \text{Br}^-, \text{I}^-$ , and  $\text{ClO}_4^-$ , are well known.<sup>5</sup> The syntheses of  $[\text{Ni}(\text{NH}_3)_6](\text{PF}_6)_2$  and its  $d_{18}$  deuteration analog were devised as follows.  $[\text{Ni}(\text{NH}_3)_6](\text{PF}_6)_2$  was prepared by the metathetical replacement reaction between  $[\text{Ni}(\text{NH}_3)_6]\text{Cl}_2$  (in an ammoniacal

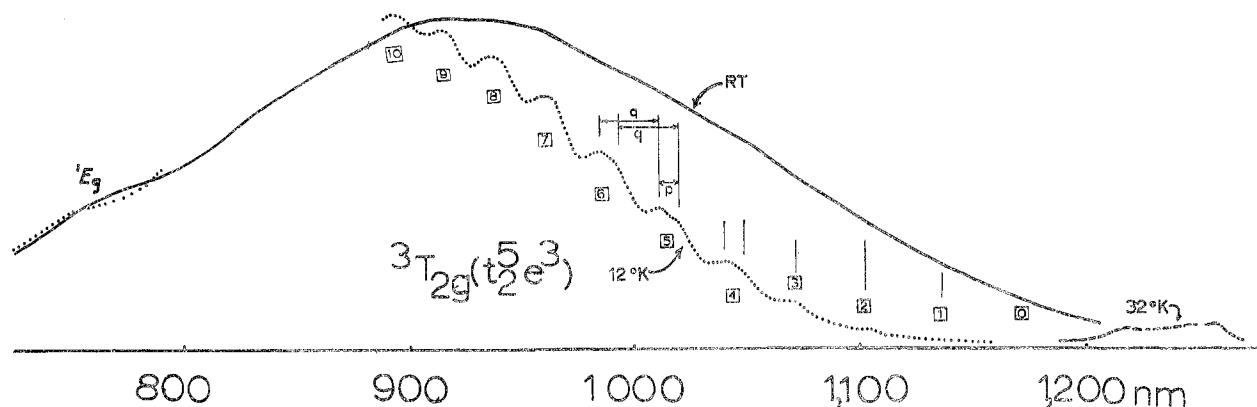


Figure 1. Electronic absorption bands,  ${}^3T_{2g}(t_{2g}^5e_g^3)$  and  ${}^1E_g(t_{2g}^6e_g^2)$ , at ambient room temperature, 32°K, and 12°K, of  $[\text{Ni}(\text{NH}_3)_6]\text{Cl}_2$  (KBr disk).

solution) and  $\text{NH}_4\text{PF}_6$ . The deep blue precipitate appeared immediately, was filtered, and then washed several times with a ca. 3% ammonia solution to remove any remaining chloride salts. This step is followed by two washes, each with absolute ethanol and diethyl ether. The reaction is nearly quantitative.

The deuterated analog,  $[\text{Ni}(\text{ND}_3)_6](\text{PF}_6)_2$ , was prepared from anhydrous  $\text{NiCl}_2$ ,  $\text{KPF}_6$ , and  $\text{ND}_4\text{OD}$  as follows. Anhydrous  $\text{NiCl}_2$  (0.01 mol), prepared *in situ* from  $[\text{Ni}(\text{H}_2\text{O})_6]\text{Cl}_2$  by heating, was dissolved in a minimum amount of  $\text{D}_2\text{O}$ . This solution was filtered into a previously filtered and saturated solution of  $\text{KPF}_6$  (0.02 mol, 3.683 g) in  $\text{D}_2\text{O}$ . To this cloudy, yellow-green solution 7 ml of 25%  $\text{ND}_3\text{-D}_2\text{O}$  in  $\text{D}_2\text{O}$  was added dropwise with stirring to produce an almost transparent, blue suspension of  $[\text{Ni}(\text{ND}_3)_6](\text{PF}_6)_2$ . The reaction mixture was allowed to cool on ice for 25 min and was then filtered. The supernatant was nearly colorless, indicating the completeness of the reaction. The precipitate was carefully washed with 2 ml of 25%  $\text{ND}_4\text{OD}$  followed by two 5-ml portions of 2.5%  $\text{ND}_4\text{OD}$ . Finally, the precipitate was washed twice, each time with absolute ethanol and diethyl ether. The reaction was nearly quantitative, and the product was at least 90% deuterated on the basis of the vibrational spectra in the N-H and N-D stretching regions, *i.e.*, 3400 and 2450  $\text{cm}^{-1}$ , respectively. The product was stored in an inert atmosphere (absence of  $\text{H}_2\text{O}$ ).

## Results and Discussion

The spectral data will be discussed in the order of increasing energy of d-d bands, which is believed<sup>2,6</sup> to be  ${}^3T_{2g}(t_{2g}^5e_g^3) < {}^1E_g(t_{2g}^6e_g^2) < {}^3T_{1g}(t_{2g}^5e_g^3) < {}^1A_{1g}(t_{2g}^6e_g^2) < {}^1T_{2g}(t_{2g}^4e_g^4) < {}^1T_{1g}(t_{2g}^5e_g^3)$ . We refer to these as bands 1, 2, 3, 4, 5, and 6, respectively. Of these bands, the first three ( ${}^3T_{2g}$ ,  ${}^1E_g$ ,  ${}^3T_{1g}$ ) were previously observed,<sup>3</sup>  ${}^1A_{1g}$  and  ${}^1T_{2g}$  were observed<sup>2</sup> in 1973, and  ${}^1T_{1g}$  is reported here for the first time.<sup>13</sup>

**Band 1, or  ${}^3A_{2g}(t_{2g}^6e_g^2) \rightarrow {}^3T_{2g}(t_{2g}^5e_g^3)$ .** This band is the lowest energy spin-allowed, one-electron d-d excitation of the interconfigurational type where an electron is excited from a nonbonding to an antibonding orbital, and its maximum is at ca. 900 nm ( $\sim 11,100 \text{ cm}^{-1}$ ) for  $[\text{Ni}(\text{NH}_3)_6]\text{Cl}_2$  (Figure 1), as measured in a KBr disk. The band of the complex with this particular  $\text{Cl}^-$  counterion will be discussed, because it showed the most vibronic structure. On lowering the temperature from ambient room temperature to 12°K there is a severe loss of intensity in the red tail, *i.e.*, from ca. 1200 nm ( $\sim 8330 \text{ cm}^{-1}$ ) to 900 nm ( $\sim 11,100 \text{ cm}^{-1}$ ), and the spectra of both temperatures are given in Figure 1. It is also quite interesting that at 12°K an extended 10-member progression develops between 1150 nm ( $\sim 8700 \text{ cm}^{-1}$ ) and 920 nm ( $\sim 10,900 \text{ cm}^{-1}$ ). The members are separated by an average of ca. 280  $\text{cm}^{-1}$ , for which reason they are assigned as advanced members of the  $a_{1g}$  skeletal  $\text{NiN}_6$  mode, where the prime symbolizes that it is the vibration in the  ${}^3T_{2g}$  electronic excited state. The reduction from the value (360  $\text{cm}^{-1}$ ) of the fundamental  $a_{1g}$  skeletal frequency<sup>2</sup> of the electronic ground state,  ${}^3A_{2g}$ , is attributed to the more antibonding nature of the excited configuration,  $t_{2g}^5e_g^3$ .

This progression has another very interesting feature; *i.e.*, the progression members at 990 nm (10,100  $\text{cm}^{-1}$ ), 1015 nm (9850  $\text{cm}^{-1}$ ), and perhaps 1045 nm (9570  $\text{cm}^{-1}$ ) are composed of two components each with a separation,  $p$ , of 80  $\text{cm}^{-1}$ . Since this value is approximately the difference in energy between  $\text{NiN}_6$  skeletal vibrational fundamentals  $t_{1u}^a$  and  $t_{1u}^b$  of the excited state  ${}^3T_{1g}(t_{2g}^5e_g^3)$ , or band 3 (*vide infra*), which is of the same antibonding excited configuration, we also attribute these pairs to  $t_{1u}^a$  and  $t_{1u}^b$  modes of the  ${}^3T_{2g}$  excited state. The consequence, then, of the presence of these two-component members is that the  $a_{1g}$  progression giving rise to the ten members is actually originating at two ungerade, single-quantum origins. The  $0 \rightarrow 0'$  origin of these progressions can be estimated by observing the positions of the hot bands which develop in the spectrum as the sample temperature is raised from 12 to 32°K (Figure 1); these are the bands at ca. 1215 nm (8230  $\text{cm}^{-1}$ ) and 1255 nm (7970  $\text{cm}^{-1}$ ), the former being broad and the latter having two components which are separated by ca. 80  $\text{cm}^{-1}$ . We note parenthetically that this last separation is about the difference between the  $t_{1u}^a$  (215  $\text{cm}^{-1}$ ) and  $t_{1u}^b$  (336  $\text{cm}^{-1}$ ) estimate; *vide infra*  $\text{NiN}_6$  skeletal fundamental modes. From these hot bands we estimate that the  $0 \rightarrow 0'$  position of  ${}^3A_{2g} \rightarrow {}^3T_{2g}$  is near  $11,700 \pm 5 \text{ nm}$  (Figure 1). More detailed spectral refinements must await the measurements on single crystals of this solid. Finally, the absorption band of Figure 1 near 750 nm (13,330  $\text{cm}^{-1}$ ), or  ${}^1E_g$ , will be discussed next.

**Band 2, or  ${}^3A_{2g}(t_{2g}^6e_g^2) \rightarrow {}^1E_g(t_{2g}^6e_g^2)$ .** This excitation at about 750 nm (13,330  $\text{cm}^{-1}$ ) (Figures 1 and 2) is spin forbidden and parity forbidden by electric dipole selection rules, but it can become allowed *via* spin-orbit coupling plus vibronic coupling to  $\text{NiN}_6$  skeletal (or N-H) vibrational modes of the excited state, *e.g.*

$$\langle \Gamma_{5g}({}^3A_{2g}) | \Gamma_{4u} | \Gamma_{3g}({}^1E_g) \cdot t_{1u}(\nu) \rangle \epsilon \Gamma_{1g}$$

$$\langle \Gamma_{5g}({}^3A_{2g}) | \Gamma_{4u} | \Gamma_{3g}({}^1E_g) \cdot t_{2u}(\nu) \rangle \epsilon \Gamma_{1g}$$

where  $\Gamma_{1g}$ , the totally symmetric representation must be contained in the direct product of the integrand, and, for example,  $\Gamma_{3g} \cdot t_{1u}(\nu)$ , symbolizes the symmetry product of the  $\Gamma_{3g}$  electronic state and a  $t_{1u}$  vibration of that state. Furthermore, one expects that the energies of the vibrational modes of this excited state,  ${}^1E_g$ , should differ very little from those of the electronic ground state because both states arise from the same spatial electron configuration,  $t_{2g}^6e_g^2$ . The distinct  $f$  progression observed (Figure 2) on  ${}^1E_g$  at 750 nm (13,330  $\text{cm}^{-1}$ ) is composed of eight members when the  $\text{PF}_6^-$  salt is studied, and it appears at 80°K. The progression was not present in the chloride salt (Figure 1). These progression members are separated by approximately  $245 \pm 10 \text{ cm}^{-1}$ . Our laser Raman spectrum of this powdered complex has a strong band at 220

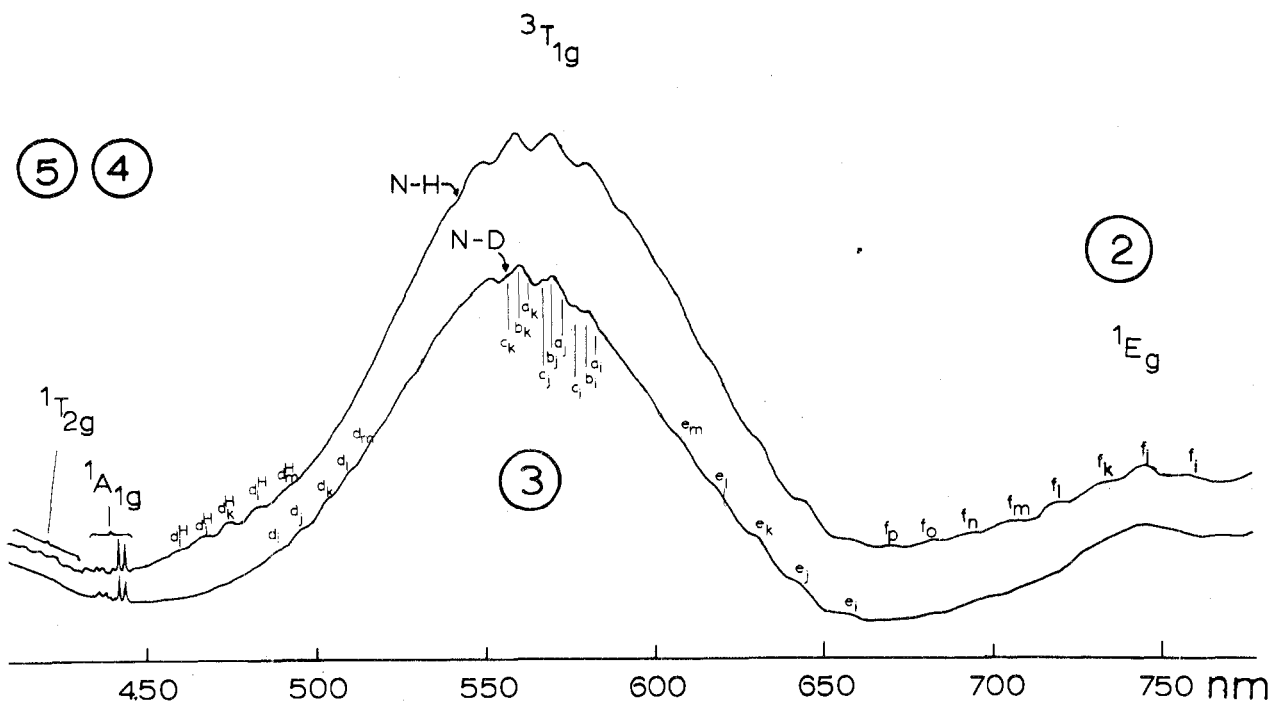


Figure 2. Electronic absorption of  ${}^1E_g$  (band 2),  ${}^3T_{1g}(t_{2g}^5e_g^3)$  (band 3), and band 4 at 80°K of  $[\text{Ni}(\text{NH}_3)_6](\text{PF}_6)_2$  and the deuterated  $d_{18}$  analog (mull).

$\text{cm}^{-1}$ , which we assign to the  $e_g$  fundamental mode of the  $\text{NiN}_6$  skeleton. For this reason one associates the eight-member progression on  ${}^1E_g(t_{2g}^6e_g^2)$  with this  $e_g$  skeletal mode. This is an unusual event, since progressions on electronic absorption bands of the  $g \rightarrow g$  type conventionally display  $a_{1g}$  progressions. We make the assignments as shown for the  $f$  progression ( $k$

$f_i$	13,193 $\text{cm}^{-1}$ (758 nm)	$t_{u'} + ke_g'$
$f_j$	13,423 $\text{cm}^{-1}$ (745 nm)	$t_{u'} + (k+1)e_g'$
$f_k$	13,661 $\text{cm}^{-1}$ (732 nm)	$t_{u'} + (k+2)e_g'$
$f_l$	13,937 $\text{cm}^{-1}$ (717.5 nm)	$t_{u'} + (k+3)e_g'$
$f_m$	14,184 $\text{cm}^{-1}$ (705 nm)	$t_{u'} + (k+4)e_g'$
$f_n$	14,440 $\text{cm}^{-1}$ (692.5 nm)	$t_{u'} + (k+5)e_g'$
$f_o$	14,684 $\text{cm}^{-1}$ (681 nm)	$t_{u'} + (k+6)e_g'$
$f_p$	14,925 $\text{cm}^{-1}$ (670 nm)	$t_{u'} + (k+7)e_g'$

= integer). It cannot be determined at this stage upon which ungerade vibration,  $t_{1u}^a$ ,  $t_{1u}^b$ , or  $t_{2u}$ , the progression is built.

**Band 3, or  ${}^3A_{2g}(t_{2g}^6e_g^2) \rightarrow {}^3T_{1g}(t_{2g}^5e_g^3)$ .** The spin-allowed, but parity-forbidden band at ca. 560 nm ( $\sim 18,000 \text{ cm}^{-1}$ ) is the result of exciting an electron from a nonbonding  $t_{2g}$  orbital to an antibonding  $e_g$  orbital. It was found that at 80°K  $[\text{Ni}(\text{NH}_3)_6](\text{PF}_6)_2$  and its  $d_{18}$  analog gave the best resolved structure (Figure 2) of the hexaammine salts studied, which included the counterions  $\text{PF}_6^-$ ,  $\text{ClO}_4^-$ ,  $\text{Cl}^-$ ,  $\text{Br}^-$ , and  $\text{I}^-$ . Five vibronic progressions are clearly visible in the spectrum of this  $\text{PF}_6^-$  salt (Table I, Figure 2). For example, on the band maximum of the  $d_{18}$  complex, the members of the  $b$  progression are most intense, and they have an average spacing of  $311 \pm 10 \text{ cm}^{-1}$ . Since the excited state,  ${}^3T_{1g}$ , is of a more antibonding configuration,  $t_{2g}^5e_g^3$ , as is  ${}^3T_{2g}$  (band 1), than the ground-state configuration,  $t_{2g}^6e_g^2$ , these members are assigned to vibronic combination levels of one quantum of an excited state  $t_{1u}^b \text{ NiN}_6$  skeletal mode and multiple quanta of the  $a_{1g}'$  skeletal mode, which in the ground state we found to be at  $348 \text{ cm}^{-1}$  in the laser Raman spectrum; the Raman and electronic spectra

Table I. Vibronic Progressions<sup>a</sup> on  ${}^3T_{1g}(t_{2g}^5e_g^3)$  of  $[\text{Ni}(\text{ND}_3)_6](\text{PF}_6)_2$  at 80°K

Resolved progressions	Position, $\text{cm}^{-1}$ (nm)	Broad progressions	Position, $\text{cm}^{-1}$ (nm)
$a_i$	17,153 (583)	$d_m$	19,608 (510)
$a_j$	17,452 (573)	$d_l$	19,908 (502.3)
$a_k$	17,778 (562.5)	$d_k$	20,202 (495)
$b_i$	17,227 (580.5)	$d_j$	20,502 (487.75)
$b_j$	17,535 (570.3)	$d_i$	20,777 (481.3)
$b_k$	17,849 (560.3)	$e_i$	15,221 (657)
$c_i$	17,331 (576.3)	$e_j$	15,552 (643)
$c_j$	17,637 (567)	$e_k$	15,860 (630.5)
$c_k$	17,963 (556.7)	$e_l$	16,155 (619)
		$e_m$	16,447 (608)

<sup>a</sup> Average spacing:  $a$ ,  $313 \text{ cm}^{-1}$ ;  $b$ ,  $311 \text{ cm}^{-1}$ ;  $c$ ,  $316 \text{ cm}^{-1}$ ;  $d$ ,  $339 \text{ cm}^{-1}$ ;  $e$ ,  $302 \text{ cm}^{-1}$ ; with an approximately  $10 \text{ cm}^{-1}$  experimental uncertainty.

were each recorded in the powdered crystalline state. The observation of relative magnitudes,  $a_{1g}'$  ( $311 \text{ cm}^{-1}$ ;  ${}^3T_{1g}$ ) <  $a_{1g}$  ( $348 \text{ cm}^{-1}$ ;  ${}^3A_{2g}$ ), is quite reasonable, and we assign (*vide infra*) the  $b$  progression as shown (see Table I).

$$\begin{aligned} b_i & t_{1u}^b{}^a + na_{1g}' \\ b_j & t_{1u}^b{}^a + (n+1)a_{1g}' \\ b_k & t_{1u}^b{}^a + (n+2)a_{1g}' \end{aligned}$$

The members of progression  $c$  (Table I, Figure 2) are on the average about  $105 \text{ cm}^{-1}$  higher in energy than the members of progression  $b$ . However, the members of progression  $c$  are separated from each other by  $316 \text{ cm}^{-1}$  which, within the experimental uncertainty, is the same spacing as between the members of progression  $b$  ( $311 \text{ cm}^{-1}$ ). Therefore, the  $a_{1g}' \text{ NiN}_6$  skeletal mode of this electronic excited state,  ${}^3T_{1g}$ , is con-

tributing to this c progression too. Also, it is known that the higher energy  $t_{1u}$  skeletal vibration,  $t_{1u}^b$  ( $\sim 330$   $\text{cm}^{-1}$ ), of the ground state is  $\sim 115$   $\text{cm}^{-1}$  higher than the one at lower energy,  $t_{1u}^a$  ( $\sim 215$   $\text{cm}^{-1}$ ). For this reason the c-progression is assigned to be based on one quantum of  $t_{1u}^b$ , where the prime signifies the vibrational mode in the  ${}^3T_{1g}$  excited state (Table I).

$$\begin{aligned} c_i & t_{1u}^b + n a_{1g}' \\ c_j & t_{1u}^b + (n+1) a_{1g}' \\ c_k & t_{1u}^b + (n+2) a_{1g}' \end{aligned}$$

The members of the third, or a progression, near the  ${}^3T_{1g}$  maximum, are weakest of the three progressions. They lie on the average 76  $\text{cm}^{-1}$  to lower energy than members of the most intense b progression. First, we find that the members of this a progression are separated (313  $\text{cm}^{-1}$ ) by the same distance within the approximate 10  $\text{cm}^{-1}$  experimental uncertainty as found for progressions b and c, so that  $a_{1g}'$  is operative again. Furthermore, it is known for similar octahedral complex ions that  $t_{2u}$   $\nu(\text{ML}_6)$  skeletal modes are at lower energy than the lowest energy  $t_{1u}$  skeletal mode. For example, we have the data shown here.

	$t_{1u}^a$	$t_{2u}$	Ref
$[\text{Cr}(\text{NH}_3)_6]^{3+}$	264 $\text{cm}^{-1}$	212 $\text{cm}^{-1}$	7a, 12
$[\text{Ni}(\text{H}_2\text{O})_6]^{2+}$	268 $\text{cm}^{-1}$	124 $\text{cm}^{-1}$	7b
$[\text{Co}(\text{H}_2\text{O})_6]^{2+}$	261 $\text{cm}^{-1}$	133 $\text{cm}^{-1}$	7b

This prompts us to assign the base of the origin of the a progression to  $t_{2u}$ . Additional and more direct evidence for  $t_{2u}$  is that we find a band at 160  $\text{cm}^{-1}$  in the far-infrared spectrum of  $[\text{Ni}(\text{NH}_3)_6](\text{ClO}_4)_2$ ; this position is 62  $\text{cm}^{-1}$  to lower energy of the  $t_{1u}^a$  far-infrared band. This difference compares very favorably with the experimental difference of 76  $\text{cm}^{-1}$  between progression members  $b_i$  ( $t_{1u}^a$ ) and  $a_i$  ( $t_{2u}$ ). This vibronic structure, then, leads to the interesting conclusion that in the  ${}^3T_{1g}(t_{2g}^2e_g^3)$  excited state the  $t_{2u}$   $\text{NiN}_6$  skeletal mode occurs about 76  $\text{cm}^{-1}$  below that of the  $t_{1u}^a$  skeletal mode (Table I).

$$\begin{aligned} a_i & t_{2u} + n a_{1g}' \\ a_j & t_{2u} + (n+1) a_{1g}' \\ a_k & t_{2u} + (n+2) a_{1g}' \end{aligned}$$

The question of where one of the  $0({}^3A_{2g}) \rightarrow 0'({}^3T_{1g})$  positions (there can be more than one since the spin-orbit manifold of  ${}^3T_{1g}$  is composed of  $\Gamma_1, \Gamma_3, \Gamma_4, \Gamma_5$ ) ought to be can be answered with somewhat reasonable certainty by analyzing the d progression (Figure 2) in the blue tail of  ${}^3T_{1g}$  along with the apparent beginning of progressions a, b, and c. Regarding the d progression observed at 80°K, it should be noted that the first observed member,  $d_i$ , at 481.3 nm (20,777  $\text{cm}^{-1}$ ) in  $d_{18} [\text{Ni}(\text{NH}_3)_6]^{2+}$ , or  $[\text{Ni}(\text{ND}_3)_6](\text{PF}_6)_2$ , is measured to be ca. 880  $\text{cm}^{-1}$  lower in energy than the first component,  $d_i^H$ , at 21,657  $\text{cm}^{-1}$  (Figure 2) of the undeuterated complex,  $[\text{Ni}(\text{NH}_3)_6](\text{PF}_6)_2$ ;  $d^H$  and d symbolize analogous progression members of  $[\text{Ni}(\text{NH}_3)_6](\text{PF}_6)_2$  and  $[\text{Ni}(\text{ND}_3)_6](\text{PF}_6)_2$ . In fact each member between 460 and 500 nm (21,750 and 20,000  $\text{cm}^{-1}$ ) of the  $d^H$  progression of  $[\text{Ni}(\text{NH}_3)_6](\text{PF}_6)_2$  shifts to lower energy by ca. 900  $\text{cm}^{-1}$  upon deuterating the complex to  $[\text{Ni}(\text{ND}_3)_6](\text{PF}_6)_2$ , i.e.,  $d_i^H - d_i = 880$   $\text{cm}^{-1}$ ,  $d_i^H - d_j = 900$   $\text{cm}^{-1}$ , etc. Indeed, this is the shift expected if the vibronic d progression consists of a symmetric N-H (N-D) stretching mode being built upon one quantum of an allowing mode  $t_{1u}^a, t_{1u}^b$ , or  $t_{2u}$  within  ${}^3T_{1g}$ .

In order to shed additional light on this possibility we obtained the following vibrational data. We find  $\nu_s^H(\text{NH}_3)$  3310  $\text{cm}^{-1}$  for  $[\text{Ni}(\text{NH}_3)_6](\text{PF}_6)_2$  and  $\nu_s^D(\text{ND}_3)$  2410  $\text{cm}^{-1}$  for the  $d_{18}$  analog from ambient room-temperature Raman spectra.

This difference,  $\nu_s^H - \nu_s^D$ , is 900  $\text{cm}^{-1}$  and our average vibronic shift,  $d^H - d$ , of 890  $\text{cm}^{-1}$  compares quite favorably with this.

The second point of interest is that the members of the d progression of  $[\text{Ni}(\text{ND}_3)_6](\text{PF}_6)_2$  are separated by an average of  $300 \pm 10$   $\text{cm}^{-1}$ . Since this is also the amount by which the members within the a, b, and c progressions are separated, it is concluded that progression members  $d_i$  to  $d_m$  are multiply excited quanta of the  $a_{1g}' \nu(\text{NiN}_6)$  skeletal vibrations. Therefore, one is led to make the assignments for the d progression as shown (Table I), where  $\Lambda$  is an integer.<sup>8</sup>

$$\begin{aligned} d_m & 1t_{u'} + \nu_s'(\text{ND}_3) + \Lambda a_{1g}'(\text{NiN}_6) \\ d_l & 1t_{u'} + \nu_s'(\text{ND}_3) + (\Lambda+1) a_{1g}'(\text{NiN}_6) \\ d_k & 1t_{u'} + \nu_s'(\text{ND}_3) + (\Lambda+2) a_{1g}'(\text{NiN}_6) \\ d_j & 1t_{u'} + \nu_s'(\text{ND}_3) + (\Lambda+3) a_{1g}'(\text{NiN}_6) \\ d_i & 1t_{u'} + \nu_s'(\text{ND}_3) + (\Lambda+4) a_{1g}'(\text{NiN}_6) \end{aligned}$$

Using converse reasoning one can now look for the  $t_{u'}$  level on which the  $\nu_s^D(\text{ND}_3)$  mode might be built; i.e., if one adds  $\nu_s^D(\text{ND}_3)$  2410  $\text{cm}^{-1}$  to the most prominent member, or  $t_{1u}^a$ , at 580.5 nm (17,227  $\text{cm}^{-1}$ ), one obtains 509 nm (19,637  $\text{cm}^{-1}$ ), which indeed is the position of the  $m$ th member (510 nm) of the d progression! This then leads to the reasonable conclusion that the  $0 \rightarrow 0'$  origin of progressions a, b, and c may be one fundamental vibrational mode of  $t_{1u}^a$  toward the red side of 580.5 nm (17,227  $\text{cm}^{-1}$ ). An estimate of this position is obtainable by reducing the  $\nu(t_{1u}^a)$  ground-state skeletal fundamental by the amount (13%) that  $a_{1g}$  of the ground state is reduced compared to  $a_{1g}'$  of the excited state,  ${}^3T_{1g}$ . Based on this reasoning, the  $0 \rightarrow 0'$  position is at 586.8 nm (17,040  $\text{cm}^{-1}$ ). We attribute this origin to the forbidden transition from  $[\Gamma_5({}^3A_{2g})]$  to  $[\Gamma_3({}^3T_{1g})]$  or  $[\Gamma_5({}^3T_{1g})]$ , or to both, because we previously ascertained, by computation<sup>2</sup> as did Liehr and Ballhausen,<sup>6</sup> that they are separated by only about 100  $\text{cm}^{-1}$ . However, this origin is speculative at present because there is another origin near about 660 nm (Figure 2) which is too far from the  $\Gamma_3, \Gamma_5$  position; i.e., a  $\Gamma_1({}^3T_{1g})$  origin near 670 nm would require the unorthodox postulate that  $\{3d(\text{Ni}^{2+})$  of the complex be sizably larger than the free-ion value of 630  $\text{cm}^{-1}$ . Thus, locating the  $\Gamma_3, \Gamma_5$  origin with greatest firmness must await the single-crystal data.

The vibronic e progression on the red tail of  ${}^3T_{1g}$  of  $[\text{Ni}(\text{ND}_3)_6](\text{PF}_6)_2$  has its members (Table I) separated by an average of 300  $\text{cm}^{-1}$ , and it starts at about 15,220  $\text{cm}^{-1}$  (657 nm). Each of these e members is broad, so that it is not possible to establish onto which of the ungerade fundamental modes,  $t_{1u}'$  or  $t_{2u}'$ , it is built. However, this 300  $\text{cm}^{-1}$  interval prompts us to assign the members to multiply excited quanta of  $a_{1g}'$  as found for the other four progressions (Table I) where

$$\begin{aligned} e_i & 1t_{u'} + \nu a_{1g}' & e_l & 1t_{u'} + (\nu+3) a_{1g}' \\ e_j & 1t_{u'} + (\nu+1) a_{1g}' & e_m & 1t_{u'} + (\nu+4) a_{1g}' \\ e_k & 1t_{u'} + (\nu+2) a_{1g}' & & \end{aligned}$$

$\nu$  is an integer. The  $0 \rightarrow 0'$  spin-orbit parentage position of this progression is difficult to estimate since it is strongly forbidden, but the spin-orbit parent ought to be  $\Gamma_1({}^3T_{1g})$  on the basis of previous ligand field computations.<sup>2,6</sup>

From Figure 2 it is evident that the general features of the vibronic structure of this  ${}^3T_{1g}$  band of  $[\text{Ni}(\text{ND}_3)_6](\text{PF}_6)_2$ , as discussed in the preceding paragraphs, are also present in the undeuterated complex,  $[\text{Ni}(\text{NH}_3)_6](\text{PF}_6)_2$ . However, most members of the progressions are broader in the latter complex, and the d progression is blue shifted for the reason given above.

The ambient room-temperature MCD solution spectrum of  $[\text{Ni}(\text{NH}_3)_6]^{2+}$  was measured by Harding, Mason, Robbins, and Thomson.<sup>4</sup> The excitation under discussion here,  ${}^3A_{2g} \rightarrow {}^3T_{1g}$ , was found to have residual integrated MCD activity.

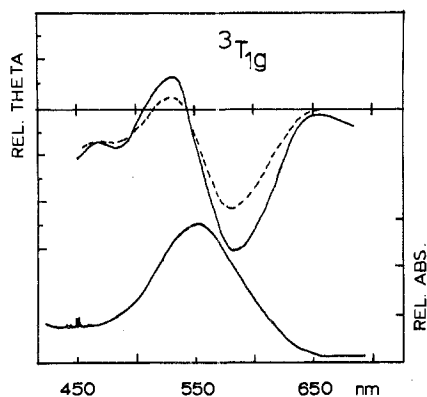


Figure 3. MCD of  ${}^3T_{1g}(t_{2g}^5e_g^3)$  at 18°K (solid line) and 27°K (dashed line) of  $[\text{Ni}(\text{NH}_3)_6]\text{Cl}_2$  (KBr disk). Electronic spectrum at 38°K.

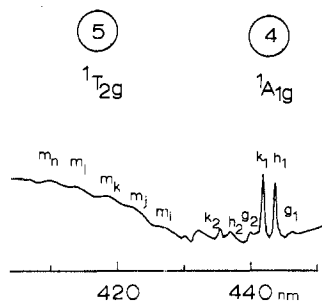


Figure 4. Electronic absorption of  ${}^1A_{1g}$  and  ${}^1T_{2g}$  (bands 4 and 5) at 80°K of  $[\text{Ni}(\text{NH}_3)_6](\text{PF}_6)_2$  (mull).

If the residual activity could be shown to be the result of Faraday *C* terms,<sup>9</sup> one could conclude that the ground state,  ${}^3A_{2g}$ , contains angular momentum (after spin-orbit coupling) from primarily the first excited state,  ${}^3T_{2g}(t_{2g}^5e_g^3)$ .<sup>10</sup> The temperature dependence of the MCD of this  ${}^3T_{1g}$  band (*ca.* 550 nm) of  $[\text{Ni}(\text{NH}_3)_6]\text{Cl}_2$ , which we measured at 18 and 27°K (Figure 3), provides the necessary experimental verification that second-order spin-orbit coupling indeed mixes angular momentum from excited state (probably  ${}^3T_{2g}$ ) into ground state,  ${}^3A_{2g}$ . It is also quite interesting to note that the negative MCD band at about 480 nm ( $20,830\text{ cm}^{-1}$ ) demonstrates that the vibronic d progression, which involves the symmetric N-H stretching motion, of this  ${}^3T_{1g}$  state has its own distinct MCD activity.

**Band 4, or  ${}^3A_{2g}(t_{2g}^6e_g^2) \rightarrow {}^1A_{1g}(t_{2g}^6e_g^2)$ .** This high-energy intraconfigurational d-d band is at about 445 nm ( $22,470\text{ cm}^{-1}$ ). Its intensity at 80°K is rather weak (Figures 2, 4) relative to its large and broad neighbor,  ${}^3T_{1g}$  (550 nm), or band 3 (toward the red), so that a rapid spectral scan can almost lead to the loss of this very interesting structure (also see Figure 5). However, the fine structure persists distinctly for seven compounds studied, *i.e.*,  $[\text{Ni}(\text{NH}_3)_6]\text{A}_2$ , where  $\text{A}^- = \text{Cl}^-, \text{Br}^-, \text{I}^-, \text{ClO}_4^-,$  and  $\text{PF}_6^-$ , and in the deuterated complex cation with counterions  $\text{A}^- = \text{Cl}^-$  and  $\text{PF}_6^-$  (see Figures 2-5). By having obtained the spectra for the deuterated and undeuterated  $\text{Cl}^-$  and  $\text{PF}_6^-$  salts, it is clear that the progressions near 445 nm ( $22,470\text{ cm}^{-1}$ ) are to be associated with skeletal  $\text{NiN}_6$  vibrations and not with N-H stretching or  $\text{NH}_3$  distortion modes. Two vibronic progressions, h and k, are of dominant intensity in the low-temperature ( $\leq 80^\circ\text{K}$ ) spectra of the seven complexes mentioned above (Figure 5 and Table II). In two of these undeuterated complexes, however, *i.e.*, the  $\text{ClO}_4^-$  and  $\text{Cl}^-$ , and in the deuterated version of the latter, a third progression, g, is observed (Figure 5, Table II). In view of the magnitudes of the separations between the first components,  $g_1, h_1, k_1$ , of the three progressions and because of the fact that each is the

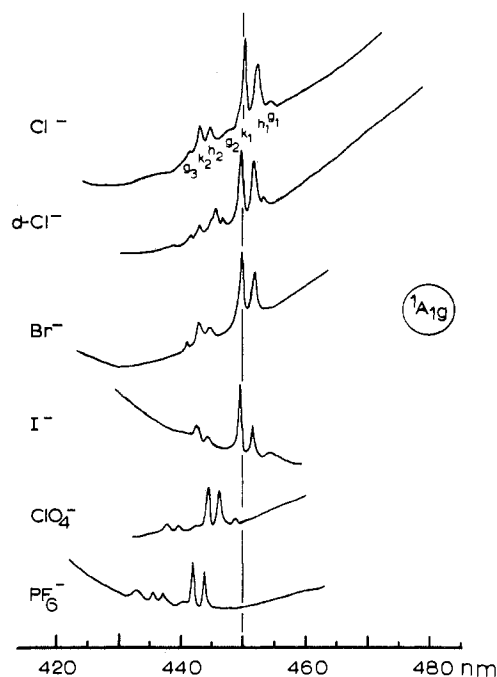


Figure 5. Electronic absorption of band 4 at 80°K of  $[\text{Ni}(\text{NH}_3)_6]\text{A}_2$  (mull). "d-Cl" is  $[\text{Ni}(\text{ND}_3)_6]\text{Cl}_2$ .

Table II. Vibronic Progressions on  ${}^1A_{1g}(t_{2g}^6e_g^2)$  of  $[\text{Ni}(\text{NH}_3)_6]\text{A}_2$  at 80°K

Member of progression	Position, $\text{cm}^{-1}$ (nm)				
	$\text{Cl}^-$	$\text{Br}^-$	$\text{I}^-$	$\text{ClO}_4^-$	$\text{PF}_6^-$
$g_1$	22,022 (454.1)			22,280 (448.8)	
$h_1$	22,112 (452.25)	22,130 (451.9)	22,153 (451.4)	22,410 (446.5)	25,530 (443.8)
$k_1$	22,209 (450.15)	22,230 (449.0)	22,247 (449.5)	22,500 (444.4)	22,620 (442.1)
$g_2$	22,346 (447.5)		22,318 (448.1)	22,619 (442.2)	22,727 (440)
$h_2$	22,471 (445.0)	22,490 (444.7)	22,490 (444.6)	22,760 (439.3)	22,870 (437.3)
$k_2$	22,578 (442.9)	22,580 (442.8)	22,580 (442.8)	22,840 (437.8)	22,960 (435.6)
$g_3$	22,676 (441.0)	22,681 (440.9)	22,648 (441.5)	22,940 (435.9)	23,094 (433)

start of an approximate  $350\text{-cm}^{-1}$  progression, we make the assignments (Table II)

$$\begin{array}{lll}
 g_1 & {}^1A_{1g} + t_{2u}' \equiv \delta & h_1 & {}^1A_{1g} + t_{1u}'^a \equiv \gamma \\
 g_2 & \delta + a_{1g}' & h_2 & \gamma + a_{1g}' \\
 g_3 & \delta + 2a_{1g}' & k_1 & {}^1A_{1g} + t_{1u}'^b \equiv \epsilon \\
 & & k_2 & \epsilon + a_{1g}'
 \end{array}$$

where all vibrations are skeletal  $\text{NiN}_6$  modes, and the positions of these bands are shown in Figure 5 (also see Table II). Also, from comparing the spectra of Figure 5 it seems the  $t_{2u}$   $\text{NiN}_6$  skeletal mode plays an intensity role only in the case of the  $\text{Cl}^-$  and  $\text{ClO}_4^-$  salts.

It is another point of interest that the energy position of the  ${}^1A_{1g}$  band depends almost linearly on the size of the unit cell of these cubic complexes. For example, Figure 6 shows our plot of the energy of the first component,  $h_1$ , of the h progression of  ${}^1A_{1g}$  as a function of the magnitude of the length of the unit cell; *i.e.*, the energy is directly proportional to the length of the unit cell. The most hydrogen-bonding halide ion,  $\text{Cl}^-$ , deviates from the linearity. It is at first sight perplexing that the energy of an intraconfigurational  $t_{2g}^6e_g^2$  excitation, such as this  ${}^3A_{2g} \rightarrow {}^1A_{1g}$  transition, should vary (Figure 6)

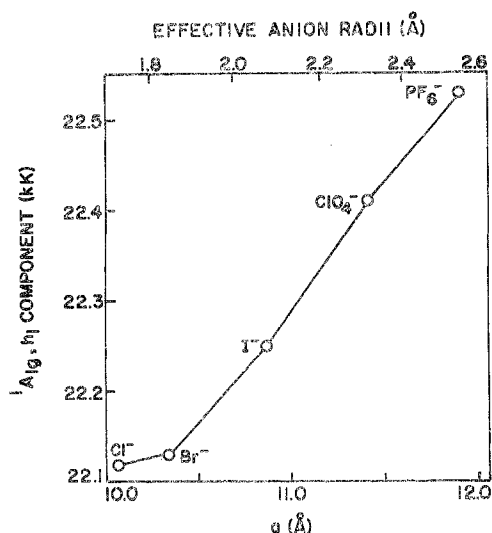


Figure 6. Variation of the position of band 4 (first component of  $h$  progression) as a function of the lengths of (cubic) unit cells and effective radii of anions.

several hundred kaysers as one changes the counterion. However, Flint and Greenough<sup>12</sup> found a similar effect in their emission spectra of  $[\text{Cr}(\text{NH}_3)_6](\text{PF}_6)_3$  and  $[\text{Cr}(\text{NH}_3)_6](\text{ClO}_4)_3$ ; *i.e.*, the intraconfiguration  $t_{2g}^3$  emission energies from  ${}^1E_g$  to the  ${}^4A_{2g}$  ground state were 15,291 and 15,221  $\text{cm}^{-1}$ , respectively. In the present study it is found, for example, that  ${}^1A_{1g}$  of the  $\text{PF}_6^-$  salt is also at higher energy than the  $\text{ClO}_4^-$  salt (22,530 and 22,410  $\text{cm}^{-1}$ ), and by the same order of magnitude. We conclude that this intraconfiguration  $t_{2g}^6e_g^2$  excitation,  ${}^3A_{2g} \rightarrow {}^1A_{1g}$  near 445 nm (22,470  $\text{cm}^{-1}$ ) is an excellent means of ascertaining the extent of interaction between the crystalline lattice and the complex ion  $[\text{Ni}(\text{NH}_3)_6]^{3+}$ . While the mechanism of interaction (hydrogen bonding or electrostatic) is less certain, hydrogen bonding appears to be a reasonable suggestion. Furthermore, if the electrostatic interaction between the lattice ion and the  $\text{Ni}^{2+}$  were dominant, then the order of energies should be  $\text{Cl}^- > \text{Br}^- > \text{I}^-$ , which contradicts our experimental order,  $\text{Cl}^- < \text{Br}^- < \text{I}^-$ .

**The Fifth and Sixth Bands,  ${}^3A_{2g} \rightarrow {}^1T_{2g}$  and  ${}^3A_{2g} \rightarrow {}^1T_{1g}$ , Respectively.** These two bands, at about 415 nm (24,100  $\text{cm}^{-1}$ ) and about 390 nm (25,640  $\text{cm}^{-1}$ ), became apparent in all our low-temperature spectra ( $\leq 80^\circ\text{K}$ ) of  $[\text{Ni}(\text{NH}_3)_6]^{2+}$  and deuterated analogs; *e.g.*, see Figures 2 and 7. The assignment of the order,  ${}^1T_{2g} < {}^1T_{1g}$ , was made on the basis of the ligand field computation ( $-Dq = 1100 \text{ cm}^{-1}$ ,  $B = 890 \text{ cm}^{-1}$ ,  $C = 3290 \text{ cm}^{-1}$ ,  $-\zeta = 400 \text{ cm}^{-1}$ ) which predicts  ${}^1T_{2g}$  (23,905  $\text{cm}^{-1}$ ) to be below  ${}^1T_{1g}$  (28,281  $\text{cm}^{-1}$ ). These computed energies can certainly be in error, since the computation does not mix the close and immensely intense charge-transfer band(s) ( $< 350 \text{ nm}$ ) with the d-d bands. At the temperature of this work only the low-energy band, or  ${}^1T_{2g}$ , showed any evidence of vibronic fine structure (Figures 2, 4). Thus, in the spectrum of  $[\text{Ni}(\text{NH}_3)_6](\text{PF}_6)_2$  at  $80^\circ\text{K}$  the following reasonably regularly spaced peaks are present

$m_i$	427.5 nm (23,392 $\text{cm}^{-1}$ )	$m_l$	414.5 nm (27,125 $\text{cm}^{-1}$ )
$m_j$	423 nm (23,641 $\text{cm}^{-1}$ )	$m_m$	410.5 nm (24,360 $\text{cm}^{-1}$ )
$m_k$	419 nm (23,866 $\text{cm}^{-1}$ )		

Since this state,  ${}^1T_{2g}$ , derives from the severely antibonding configuration  $t_{2g}^4e_g^4$ , it is reasonable to associate this spacing (*ca.* 245  $\text{cm}^{-1}$ ) with an  $a_{1g}$  progression of the excited state.

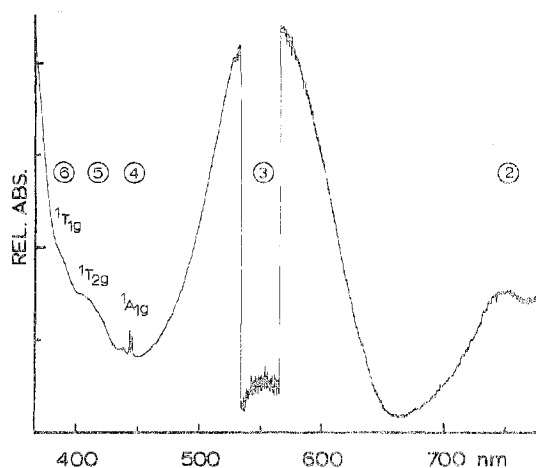


Figure 7. Electronic absorption spectrum of  $[\text{Ni}(\text{ND}_3)_6](\text{ClO}_4)_2$ , obtained at  $79^\circ\text{K}$ , which shows bands 5 and 6 (null).

### Summary

The low-temperature electronic absorption spectra of salts of  $[\text{Ni}(\text{NH}_3)_6]^{2+}$  reveal two vibronic progressions on  ${}^3T_{2g}(\text{F})$ , five progressions on  ${}^3T_{1g}(\text{F})$ , one progression on  ${}^1E_g(\text{D})$ , three progressions on  ${}^1A_{1g}(\text{G})$ , and one on  ${}^1T_{2g}(\text{D})$ . The members of these progressions variously involve excitations of  $a_{1g}$ ,  $e_g$ ,  $t_{1u}^a$ ,  $t_{1u}^b$ , and  $t_{2u}$   $\text{NiN}_6$  skeletal modes and the symmetric N-H stretching mode of coordinated  $\text{NH}_3$ . It is also found that the position of the  ${}^3A_{2g} \rightarrow {}^1A_{1g}$  intraconfigurational excitation is a good indicator of the interaction of the lattice ions and the complex ion  $[\text{Ni}(\text{NH}_3)_6]^{2+}$ . Finally, the MCD spectra as measured at two temperatures through the  ${}^3T_{1g}(\text{F})$  establish that the Faraday C term activity of this band and the presence of the residual MCD activity verify experimentally that the ground state,  ${}^3A_{2g}$ , obtains angular momentum by second-order spin-orbit coupling, probably with the  ${}^3T_{2g}(\text{F})$  excited state.

**Registry No.**  $[\text{Ni}(\text{NH}_3)_6]\text{Cl}_2$ , 10534-88-0;  $[\text{Ni}(\text{NH}_3)_6]\text{Br}_2$ , 13601-55-3;  $[\text{Ni}(\text{NH}_3)_6]\text{I}_2$ , 13859-68-2;  $[\text{Ni}(\text{NH}_3)_6](\text{ClO}_4)_2$ , 14322-50-0;  $[\text{Ni}(\text{NH}_3)_6](\text{PF}_6)_2$ , 18445-50-6;  $[\text{Ni}(\text{ND}_3)_6](\text{PF}_6)_2$ , 53385-37-8;  $[\text{Ni}(\text{ND}_3)_6](\text{ClO}_4)_2$ , 53385-38-9;  $[\text{Ni}(\text{ND}_3)_6]\text{Cl}_2$ , 14286-01-2.

### References and Notes

- (1) Acknowledgment is made to the donors of the Petroleum Research Fund, administered by the American Chemical Society, for support of this research.
- (2) A. F. Schreiner and D. J. Hamm, *Inorg. Chem.*, **12**, 2037 (1973).
- (3) C. K. Jorgensen, *Acta Chem. Scand.*, **9**, 1362 (1955); O. G. Holmes and D. S. McClure, *J. Chem. Phys.*, **26**, 1686 (1957); J. Reedijk, P. W. N. M. van Leeuwen, and W. L. Groeneveld, *Recl. Trav. Chim. Pays-Bas*, **87**, 129 (1968).
- (4) M. J. Harding, S. F. Mason, D. J. Robbins, and A. J. Thomson, *J. Chem. Soc. A*, 3058 (1971).
- (5) G. G. Schlessinger, "Inorganic Laboratory Preparations," Chemical Publishing Co., New York, N. Y., 1962, p 194.
- (6) A. D. Liehr and C. J. Ballhausen, *Mol. Phys.*, **2**, 123 (1959).
- (7) (a) T. Shimanouchi and I. Nakagawa, *Inorg. Chem.*, **3**, 1805 (1964); (b) R. G. Brown and S. D. Ross, *Spectrochim. Acta*, **26**, 945 (1970).
- (8)  $[\text{Ni}(\text{H}_2\text{O})_6]^{2+}$  appears to behave similarly during the excitation  ${}^3A_{2g} \rightarrow {}^3T_{1g}$  in that a symmetric O-H stretching mode is active along with skeletal modes. See T. S. Piper and N. Koertge, *J. Chem. Phys.*, **32**, 559 (1960).
- (9) A. D. Buckingham and P. J. Stephens, *Annu. Rev. Phys. Chem.*, **17**, 399 (1966).
- (10) R. G. Denning and J. A. Spencer, *Symp. Faraday Soc.*, **3**, 84 (1969).
- (11) Lengths of unit cells are from G. Boedtker-Naess and O. Hassel, *Z. Phys. Chem., Abt. B*, **22**, 471 (1933), for  $\text{Cl}^-$ ,  $\text{Br}^-$ ,  $\text{I}^-$ ,  $\text{ClO}_4^-$ , and from B. Boedtker-Naess and O. Hassel, *Nor. Vidensk., Acad. Oslo I. Mat. Natur. Kl., Abhandl.*, **1** (1933), for  $\text{PF}_6^-$ . The anion effective radii are from the same sources.
- (12) C. D. Flint and P. Greenough, *J. Chem. Soc., Faraday Trans. 2*, **68**, 897 (1972).
- (13) Vibrations of excited states are primed. The electronic parentage is clear from the discussion.